RSC Advances

PAPER

View Article Online
View Journal | View Issue

Cite this: *RSC Adv.*, 2024, **14**, 1593

Preconcentration and selective extraction of trace Hg(II) by polymeric g-C_3N_4 nanosheet-packed SPE column

Uzma Haseen,[a] Syed Ghazanfar Ali,[b] Rais Ahmad Khan,[c] Ali Alsalme,[c] Bon Heun Koo[d] and Hilal Ahmad *[e]

In this study, we successfully synthesized polymeric graphitic carbon nitride (g-C_3N_4) nanosheets through thermal means and proposed their application in solid-phase extraction (SPE) for the enrichment of trace Hg(II). The nanosheets underwent characterization using scanning electron microscopy, tunnelling electron microscopy, and energy-dispersive X-ray spectroscopy. The column packed with polymeric carbon nitride nanosheets demonstrated effective extraction of trace Hg(II) ions from complex samples. The g-C_3N_4 nanosheets possess a zeta potential value of −20 mV, enabling strong interaction with positively charged divalent Hg(II) ions. This interaction leads to the formation of stable chelates with the nitrogen atoms present in the polytriazine and heptazine units of the material. The proposed method exhibited a high preconcentration limit of 0.33 μg L^{-1}, making it suitable for analysing trace amounts of Hg(II) ions. Moreover, the method's applicability was confirmed through successful analysis of real samples, achieving an impressive preconcentration factor of 200. The detection limit for trace Hg(II) ions was determined to be 0.6 μg L^{-1}. To assess the accuracy of the method, we evaluated its performance by recovering spiked amounts of Hg(II) and by analysing certified reference materials. The results indicated excellent precision, with RSD consistently below 5% for all the analyses conducted. In conclusion, the thermally synthesized polymeric carbon nitride nanosheets present a promising approach for solid-phase extraction and preconcentration of trace Hg(II) from real samples. The method showcases high efficiency, sensitivity, and accuracy, making it a valuable tool for environmental and analytical applications.

Received 14th August 2023
Accepted 2nd December 2023

DOI: 10.1039/d3ra05512d

rsc.li/rsc-advances

1. Introduction

The environmental contamination of mercury ions (Hg(II)) is tagged as severe class 1 pollution.[1,2] This hazardous element poses a significant global environmental issue,[2–4] as even low levels of Hg(II) can have detrimental effects on human health.[5] Long-term exposure to Hg(II) can permanently damage the developing foetus, kidneys, and brain.[6–8] To address this concern, the US Environmental Protection Agency has set a maximum limit of 2.0 ppb for Hg(II) in consumable water, and the World Health Organisation (WHO) emphasizes the importance of monitoring and evaluating such harmful metals.[9,10] However, directly detecting trace levels of Hg(II) in natural samples is challenging using common techniques like atomic fluorescence spectrometry, X-ray fluorescence, cold vapour atomic absorption, graphite furnace atomic absorption spectroscopy, inductively coupled plasma optical emission spectroscopy, and inductively coupled plasma mass spectrometry due to elemental interferences and sampling limitations.[11,12] Real-world samples contain numerous anions and cations that are much more abundant, leading to interference in the spectral analysis.[11,13] Consequently, sample pre-treatment methods are often required to remove matrix components and enhance the sensitivity of trace metal measurement.[14–17] Among these methods, solid phase extraction (SPE) is widely employed due to its simplicity, affordability, high concentration factors, and complete recovery of analyte.[17–20] Various SPE sorbents, including nano-sorbents like cellulose nanofibers, graphene, carbon nanotubes, silica, and magnetite materials, have been effectively used for the extraction and preconcentration of heavy metal ions.[21–27] Nevertheless, with increasing sample complexity and the demand for faster analysis, the development of new sorbents remains necessary. In this study, we report for the first time on the utilization of polymeric carbon nitride (CN)

[a]*Department of Chemistry, Aligarh Muslim University, Aligarh, 202002, India*
[b]*Department of Microbiology, Jawaharlal Nehru Medical College, Aligarh Muslim University, Aligarh, 202002, India*
[c]*Department of Chemistry, College of Science, King Saud University, Riyadh 11451, Saudi Arabia*
[d]*School of Materials Science and Engineering, Changwon National University, Changwon 51140, Gyeongnam, South Korea*
[e]*Faculty of Applied Sciences, Ton Duc Thang University, Ho Chi Minh City 700000, Vietnam. E-mail: hilalahmad@tdtu.edu.vn*

nanosheets in extraction and enrichment of analytes. The graphitic-conjugated structure of CN is composed of tri-*s*-triazine repeating units.[28] Its features such as low cost, easy production, excellent physicochemical stability, metal-free composition, minimal cytotoxicity, and environmental friendliness have made CN a popular research subject.[29] The polymeric 2D sheet-like structure, superior chemical stability, and abundance in nature make CN a promising candidate for effective SPE applications. Furthermore, the graphitic, graphene-like structure with sp^2 bonds connecting carbon and nitrogen provides excellent binding sites for metal adsorption, granting CN nanosheets remarkable selectivity for Hg(II) adsorption.

In this study, we demonstrate the straightforward thermal synthesis of porous CN nanosheets using urea as the precursor, and we investigate their potential in preconcentrating trace Hg(II) ions. Heating the N-rich urea precursor initiates a combination of polyaddition and fasciculation reactions, resulting in a defect-rich, N-bridged polytriazine structure in CN.[30] The obtained CN exhibits a unique in-plane repetition of the heptazine (C_6N_7) unit, forming a stacking motif of identical heptazines on top of each other. The planar structure consists of a one-dimensional chain of N–H bridging C_6N_7 units with an amino group at the end, giving rise to a stable zigzag shape due to hydrogen bonding when the polymer chains are in proximity to one another.[31] This conjugated polymeric network ensures the high physical and chemical stability of CN.

2. Experimental

2.1. Materials and samples

Urea (purity 99.9%), was obtained from Sigma-Aldrich and used as received. All metal salts either in nitrate or chloride salts were obtained from Sigma-Aldrich and a stock solution of 1000 ppm was prepared and diluted as per experimental requirement. A 2% nitric acid was used to rinse the glass wares before use. The standard Reference Material (SRM 1641d) was obtained from National Institute of Environmental Studies (Ibaraki, Japan) and used for method validation. The tap water samples were collected from laboratory, the ground water was collected from the local area near battery manufacturing industries and sea water was collected from south part of India. The water samples were filtered through cellulose nitrate filters to removed any particulate matter and stored in a polyethylene bottle. The collected water samples have been analyzed within a week of collection.

2.1.1 Synthesis. To synthesize polymeric carbon nitride (CN), a process involving annealing urea was employed. Specifically, 5.0 grams of urea were subjected to annealing at 550 °C under an air atmosphere for a duration of 4 hours. The annealing rate was set at 5 °C per minute. Subsequently, a light-yellow g-C_3N_4 powder was obtained, which was further finely ground using a mortar and pestle. This finely ground powder was then subjected to additional calcination at 550 °C for 2 hours under an air atmosphere to achieve thermally exfoliated porous thin sheets of CN.

2.1.2 Column procedure for Hg(II) preconcentration. A glass column with dimensions of length (L) 10 cm and diameter (Dia.) 1 cm was packed with 200 mg of polymeric carbon nitride (CN). Prior to the experiment, the column was preconditioned with a buffer solution of pH 6.0 ± 0.2. To carry out the solid phase extraction (SPE) process, a peristaltic pump was utilized to push a 100 mL solution containing Hg(II) at the required concentration and pH 6.0 ± 0.2 through the column. The sample solution was passed across the CN-packed column at a flow rate of 8 mL per minute. After the extraction process, the sorbed amount of Hg(II) onto the CN nanosheets packed column was eluted using the 5 mL of 0.5 M hydrochloric acid as an stripping agent and subsequently analyzed using an inductively coupled plasma optical emission spectrometer (ICP-OES, PerkinElmer Avio 200). This analytical instrument allowed for the measurement and quantification of the Hg(II) ions that were extracted and preconcentrated from diluted samples by using the CN packed column during the solid phase extraction to analyse the Hg(II) ions.

2.2. ICP-OES operating conditions

The Inductively Coupled Plasma Optical Emission Spectrometer (ICP-OES) was operated under specific conditions to determine Hg(II) concentrations in the samples. The instrument utilized the following parameters:

Parameters	Conditions
Nebulizer	Ultrasonic
Detector	Charge-coupled detector (CCD)
Injector	Alumina injector
Plasma gas	Argon gas; flow rate: 8.0 L min^{-1}
Auxiliary gas flow rate	0.2 L min^{-1}
Nebulizer gas flow rate	0.7 L min^{-1}
Pressure	3.2 bar
Replicates	3
Integration time	10 s
Wavelength	194.168 nm
Mode of viewing plasma	Axial mode

2.3. Materials characterization

The surface morphology of g-C_3N_4 was analyzed using a Field Emission Scanning Electron Microscope (FESEM), specifically the JSM-7800F model manufactured by JEOL, Japan. For high-resolution examination of the g-C_3N_4, a TECNAI F30 S-Twin model was utilized as a Transmission Electron Microscope (TEM). Before TEM characterization, the CN sample was well dispersed in methanol and probe-sonicated to ensure a well-distributed sample. To investigate the surface elements, X-ray Photoelectron Spectroscopy (XPS) was employed. The Thermo Fisher Scientific ESCALAB 250Xi model was used for XPS analysis. A binding energy range of 0–1400 eV was employed, and a MgKα X-ray source with an energy of 1253.6 eV was used for excitation. The XPS analysis allowed for the examination of the surface elements within a detection depth of approximately 10 nanometers. By utilizing these advanced analytical techniques,

we gain valuable insights into the surface morphology, high-resolution structure, and surface elements of g-C_3N_4, contributing to a comprehensive understanding of the material's properties and potential applications.

3. Results and discussion

3.1. Characterization

The prepared polymeric carbon nitride (CN) was examined for its surface morphology by using Scanning Electron Microscopy (SEM). Fig. 1a shows a SEM image of the prepared CN, which clearly shows a layered structure of bulk CN. In Fig. 1b, a high-resolution Transmission Electron Microscopy (TEM) image of CN nanosheets is presented. The nanosheets are well exfoliated and exhibit a wrinkled surface with single to few layered arrangements. To assess the surface properties further, the Brunauer–Emmett–Teller (BET) method was employed to determine the surface area and porosity. The BET surface area was measured to be 158 m^2 g, and the porosity was found to be 0.864 cm^3. For investigating the successful adsorption of Hg(II) onto the CN surface, Energy Dispersive X-ray Spectroscopy (EDX) spectra and elemental mapping of CN after Hg(II) adsorption were conducted (Fig. 2). These analyses confirm the effective adsorption of Hg(II) onto the CN surface. Fig. 3, illustrates the FTIR and XRD spectra of prepared CN. In FTIR spectra (Fig. 3a), the characteristics broad peaks observed at 3080–3260 cm^{-1} corresponds to amine groups resides onto the edges of CN.[32] The peaks in region of 1200–1650 cm^{-1} are associated with C–N and C=N stretching vibrations of the CN aromatic units, the characteristic out of plane vibrations of triazine/s-triazine aromatic repeating units was observed at 885 and 807 cm^{-1}. In the X-ray diffraction (XRD) shown in Fig. 3b, the observed peak at approximately 26.69° can be attributed to g-C_3N_4 and is in close proximity to the peak at around 27.7°, as reported by Chang *et al.*[33] Chang *et al.* indexed the latter peak as the (002) plane, representing the long-range arrangement of stacked aromatic repeating units within polymeric CN. The zeta potential measurements were performed to understand the

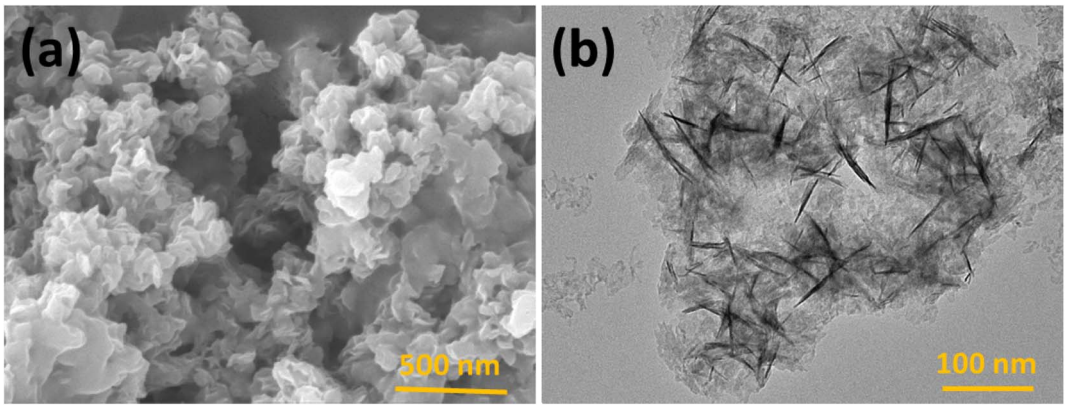

Fig. 1 (a) FESEM image and (b) HRTEM image of polymeric CN nanosheets.

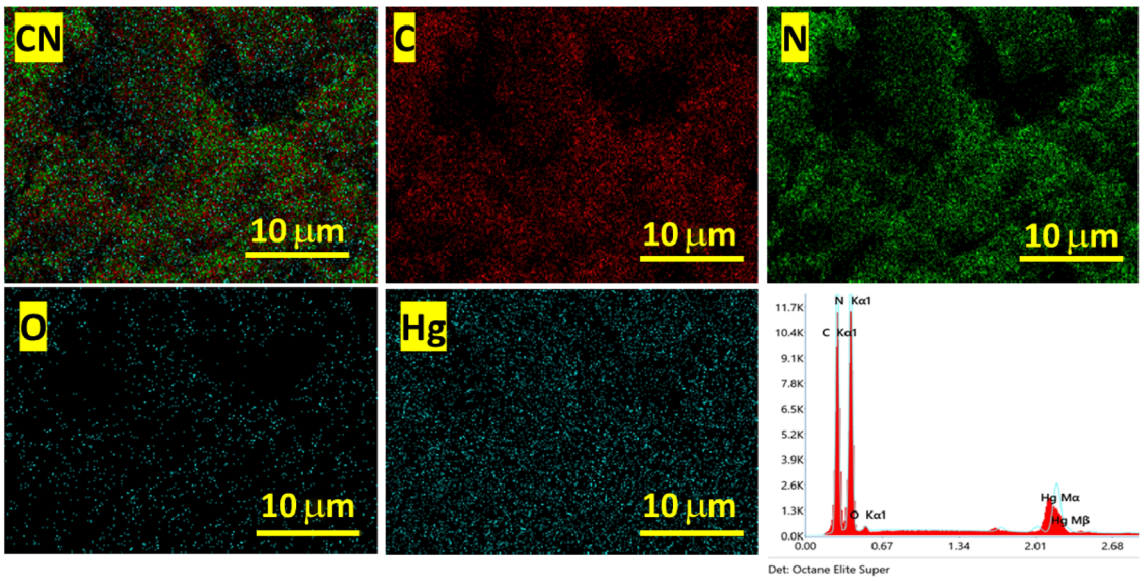

Fig. 2 EDX spectra and elemental mapping of CN after Hg(II) adsorption.

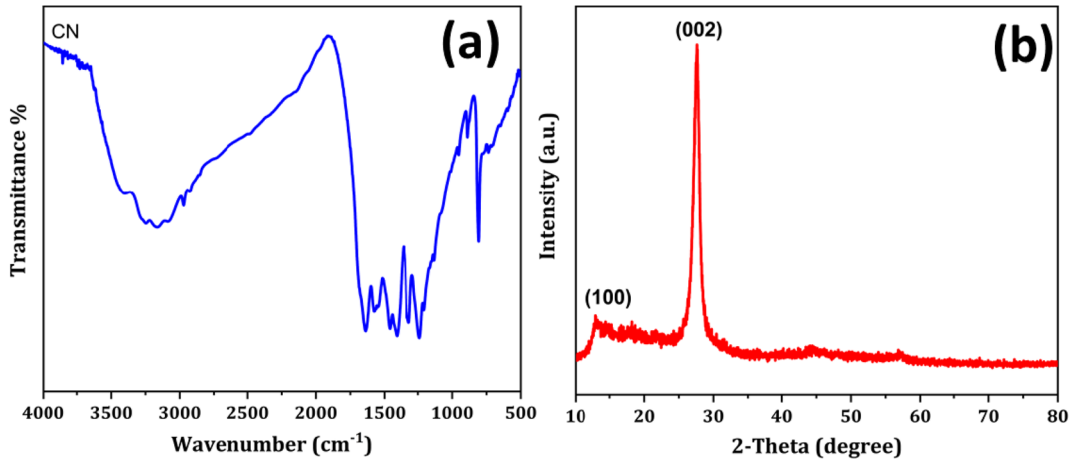

Fig. 3 (a) FTIR spectra and (b) and XRD spectra of polymeric CN.

surface charge properties of CN at different sample pH levels. Further discussion regarding these results is provided in later sections of the study. Overall, the surface characterization of the prepared CN through SEM, TEM, BET surface area, porosity, EDX, elemental mapping, and zeta potential measurements has provided valuable insights into the material's structure, adsorption capabilities, and surface charge properties, contributing to a comprehensive understanding of its potential applications.

3.2. Effect of sample pH

The pH of the solution plays a crucial role in the adsorption of metal ions onto an adsorbent, as it affects both the surface charge of the adsorbent and the chemical form of metal ions in the solution. To investigate the impact of sample pH on the adsorption of Hg(II) and other metal ions onto CN, experiments were conducted within the pH range of 1 to 7. The results are presented in Fig. 4a. It was noted that the adsorption of Hg(II) increased as the sample pH was raised from 1.0 to 7.0 (Fig. 4a). The potential binding sites for Hg(II) adsorption are the intrinsic nitrogen atoms of CN. At low sample pH, these binding sites get protonated, resulting in poor adsorption of Hg(II) in acidic media and limited sorption at low pH levels. However, as the sample pH increases, the interaction between the –N atoms and H^+ weakens, leading to enhanced adsorption of Hg(II) at higher pH levels. This behaviour is consistent with the zeta potential measurements of polymeric CN (Fig. 4b). The isoelectric point of CN was observed at pH 4.5, suggesting that the CN surface becomes negatively charged at sample pH levels beyond this value. This negative surface charge facilitates strong interactions with the positively charged Hg(II) ions, contributing to increased adsorption. The adsorption of Hg(II) onto CN is attributed to its inherent nitrogen-rich characteristics, small sheet size, and multi-layered structure with a defect-rich surface. These properties provide CN with a significant adsorption propensity towards Hg(II). Two primary hypothesized mechanisms for Hg(II) adsorption on CN include complexation with the nitrogen atoms of the polymeric CN adsorbent and electrostatic interactions.

Moreover, the presence of common cations and anions, such as Na^+, K^+, Ca^{2+}, Mg^{2+}, Cl^-, Br^-, NO^{3-}, SO_4^{2-}, and PO_4^{3-}, at concentrations significantly higher than the Hg(II) concentration did not significantly reduce the adsorption of Hg(II) onto CN (Table 1). This suggests that CN exhibits robust adsorption

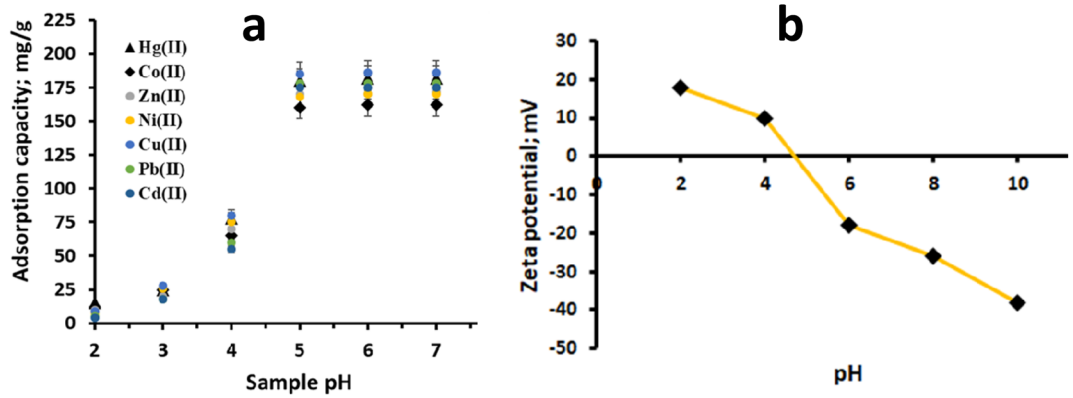

Fig. 4 (a) pH envelop of CN for Hg(II) and other heavy metal adsorption and, (b) zeta potential of polymeric CN.

Table 1 Tolerance limit of co-existing ions on the extraction of Hg(II) ions in binary mixture (experimental conditions: pH 6, total volume 50 mL; flow rate 8 mL min^{-1}, metal ions 100 μg L^{-1})

Added ions (salt used)	Tolerance ratio [added ions/metal ion]	Recovery (%)	RSD ($N = 3$)
Na^+ ($NaCl$)	5.92×10^4	98.6	4.85
K^+ (KCl)	3.45×10^4	98.8	3.66
NH_4^+ (NH_4Cl)	2.5×10^4	99.2	3.07
Ca^{2+} ($CaCl_2$)	4.75×10^4	97.4	4.00
Mg^{2+} ($MgCl_2$)	3.82×10^4	98.7	4.02
CH_3COO^- (CH_3COONa)	6.85×10^4	100.6	2.53
Cl^- ($NaCl$)	3.82×10^6	100.8	3.98
Br^- ($NaBr$)	4.65×10^6	100.5	4.46
SO_4^{2-} (Na_2SO_4)	4.50×10^5	98.9	3.64
CO_3^{2-} (Na_2CO_3)	5.30×10^5	100.2	3.86
NO_3^{2-} (Na_2NO_3)	4.80×10^5	99.4	4.05
Humic acid	250	97.0	3.54
Fulvic acid	250	99.2	3.83

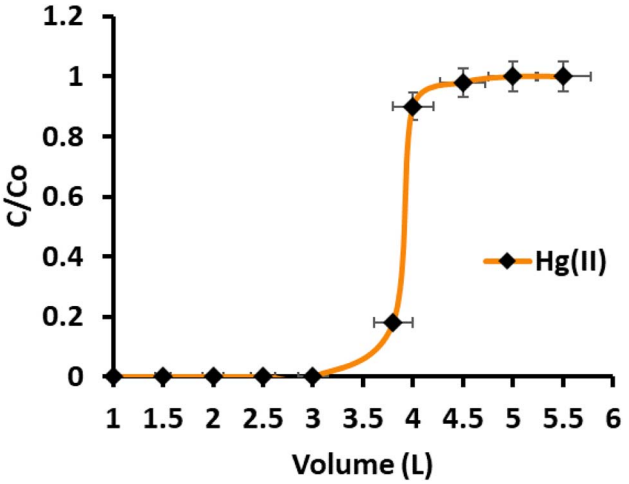

Fig. 5 Breakthrough curve for Hg(II) adsorption in continuous column operation (sample concentration 10.0 mg L^{-1}, pH 6.0, flow rate 8 mL min^{-1}).

capability for Hg(II) even in the presence of interfering ions commonly found in real samples. In conclusion, the study demonstrates that the adsorption of Hg(II) onto CN is influenced by the sample pH and is enhanced at higher pH levels due to the interaction between nitrogen atoms of CN and Hg(II) ions. CN's unique properties, including its nitrogen-rich composition, small particle size, and multi-layered structure, contribute to its excellent adsorption propensity for Hg(II) ions, making it a promising adsorbent for water treatment and environmental remediation applications. Additionally, CN's resistance to interference from other common ions enhances its potential as an effective and selective adsorbent for trace metal removal from complex real-world samples.

3.3. Preconcentration studies and breakthrough volume

The direct determination of Hg(II) in environmental samples with ultra-trace concentrations remains challenging due to the presence of co-existing anions and cations at much higher concentrations, leading to spectral interferences. Preconcentration is a valuable technique that involves transferring a small quantity of Hg(II) from a larger sample volume to a smaller volume. This process increases the analyte concentration while removing interfering ions from the pre-treated sample. In the study, model solutions containing 1.0 μg of Hg(II) were prepared at various concentrations (0.83 ppb, 0.58 ppb, 0.45 ppb, 0.37 ppb, 0.33 ppb, and 0.31 ppb) by diluting and adjusting the pH to 6.0. A peristaltic pump was used to percolate the solutions down the CN-packed column at a flow rate of 8 mL per minute. To elute the retained Hg(II), a 5 mL stripping agent was used, and the eluted Hg(II) was subsequently determined by ICP-OES. The results showed that Hg(II) was quantitatively preconcentrated up to a sample volume of 3000 mL, with a recovery of 99.5%. However, beyond a sample volume of 3000 mL, a significant decrease in adsorption was observed, resulting in a recovery of 91.7% for a sample volume of 3200 mL. The preconcentration of 1 μg of Hg(II) from a sample volume of 3000 mL was repeated three times, and the mean recovery value for all three observations was found to be 99.7%. The computed preconcentration factor and preconcentration limit for Hg(II) were determined to be 600 and 0.33 μg L^{-1}, respectively. Additionally, breakthrough studies were conducted to assess the continuous utility of the CN-packed column. The CN column was passed with sample volumes ranging from 2000 mL to 5000 mL, containing 1.0 mg L^{-1} of Hg(II). The concentration of Hg(II) in the effluent fractions was measured, and the breakthrough curve was plotted (Fig. 5). The maximum saturation capacity of CN, equivalent to the maximum sorption capacity, was calculated and found to be 176.0 mg g^{-1}. The high preconcentration factor and dynamic capacity (180.0 mg g^{-1}), which are close to the breakthrough capacity, indicate that the CN adsorbent is suitable for the column method. In summary, the preconcentration technique using the CN-packed column demonstrated effective preconcentration of ultra-trace levels of Hg(II) from large sample volumes, making it a promising approach for the sensitive determination of Hg(II) in environmental samples. The breakthrough studies further confirmed the adsorbent's suitability and high sorption capacity for this application.

3.4. Optimization of sample flow rate

The column flow rate during the sorption of Hg(II) plays a crucial role in the interaction of metal ions with binding sites and the duration of the analysis. The efficiency of the extraction process relies on the sample flow rate, as it determines the contact time between the metal ions and the chelating sites of the adsorbent bed. To investigate the effect of sorption flow rate on the adsorption of Hg(II), a 50 mL model solution containing 1.0 mg L^{-1} of Hg(II) at pH 6.0 ± 0.2 was passed through the column at different flow rates ranging from 2 to 10 mL per minute. The objective was to determine the optimal sorption flow rate for the complete adsorption of Hg(II).

The results revealed that a sample flow rate of upto 8 mL per minute shows complete adsorption of Hg(II). At these flow rates,

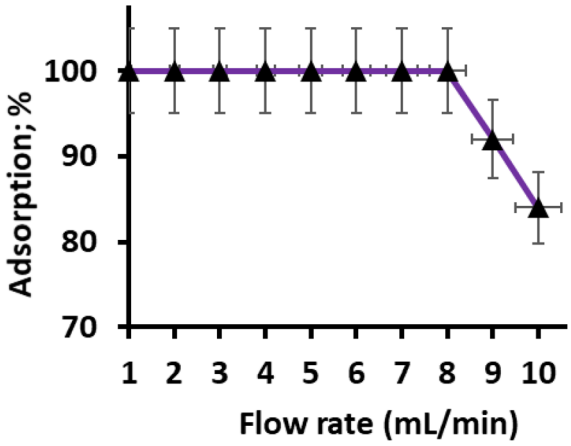

Fig. 6 Effect of sample flow rate on Hg(II) adsorption (sample volume 50 mL; sample concentration 1.0 mg L^{-1}, pH 6.0).

the metal ions effectively interacted with the chelating sites of the adsorbent bed, resulting in maximum adsorption. However, it was observed that further increasing the sample flow rate led to a gradual reduction in adsorption efficiency (Fig. 6). Based on these findings, a sorption flow rate of 8 mL per minute was selected for subsequent trials, as it provided the most efficient and complete adsorption of Hg(II) onto the CN adsorbent.

In summary, the study demonstrated that the sorption flow rate significantly influences the adsorption of Hg(II) onto the CN adsorbent. An optimal flow rate of 8 mL min^{-1} was identified to ensure effective interaction between the metal ions and the chelating sites, leading to maximum adsorption efficiency. This information is crucial for designing and optimizing the pre-concentration process for the sensitive determination of Hg(II) in real environmental samples.

3.5. Choice of eluent type and concentration

A proper eluent has been needed to completely remove out the pre-sorbed metal ions, in order to reuse the column. To achieve this, different type of acids, including hydrochloric acid, nitric acid, and sulfuric acid, were tested at different concentrations ranging from 0.25 M to 1.0 M, and different volumes of 2 mL, 3 mL, and 5 mL. The results, as depicted in Fig. 7, showed that all the tested acids at higher concentrations and varying volumes achieved quantitative recovery of Hg(II). However, at lower concentrations (0.25 M), except for 5 mL of hydrochloric acid which achieved a recovery of >99.9%, the recovery of Hg(II) was less than 90% for other acid concentrations. Based on these findings, it was determined that 5 mL of 0.5 M hydrochloric acid was the most effective eluent for regenerating the column for the subsequent sorption cycle. It provided quantitative recovery of Hg(II) and ensured complete desorption of the sorbed metal ions. In brief, the study identified 5 mL of 0.5 M hydrochloric acid as the optimal eluent to efficiently desorb and recover the sorbed Hg(II) from the CN-packed column. This eluent type and concentration allow for successful column regeneration and subsequent sorption cycles, making the method robust and suitable for continuous use in environmental sample analysis.

3.6. Analytical method validation

The validation of an analytical technique is crucial to ensure the appropriateness and reliability of the methodology in producing usable analytical results. In this study, the analytical technique for preconcentrating and determining Hg(II) using the CN-packed column was validated. The calibration plot, generated under optimal experimental conditions, exhibited excellent linearity with an R^2 correlation coefficient of 0.9998. This indicates a strong relationship between the analyte concentration and the instrumental response, confirming the accuracy of the method. The limits of detection (LOD) and quantification (LOQ) were determined by analysing 11 replicate measurements of the blank solution after passing through the CN column. The LOD and LOQ were found to be 0.06 μg L^{-1} and 0.20 μg L^{-1}, respectively. These values indicate the method's sensitivity and its ability to detect and quantify Hg(II) at low concentrations, making it suitable for real sample analysis. To assess the accuracy of the procedure, ten consecutive measurements of 1 ppb Hg(II) were performed, and the relative standard deviation (RSD) was calculated to be 2.8%. This low RSD value indicates the method's acceptable precision and the proximity of repeated observations. The accuracy of the proposed technique was further evaluated by analysing a Standard Reference Material (SRM 1641d) and real samples spiked with known concentrations of Hg(II). The results, presented in Tables 2 and 3, demonstrate a high degree of agreement between the obtained values and the certified values for the SRM, confirming the accuracy of the method. Additionally, the mean percentage recoveries for the spiked Hg(II) in real samples ranged from 98.3% to 100.8%, with an RSD of less than 5%, further validating the method's accuracy and precision. In

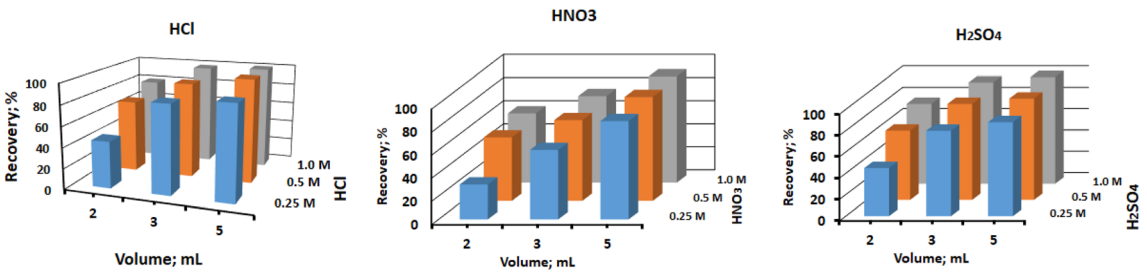

Fig. 7 Effect of eluent type, concentration and volume on the recovery of adsorbed Hg(II) ions.

Table 2 Method validation: determination of Hg(II) ions in standard reference materials (sample volume 50 mL, pH 6, sample flow rate 8 mL min^{-1}, eluent volume 5 mL (0.5 M HCl) and eluent flow rate 1 mL min^{-1})

Samples	Certified values[a] (μg g^{-1})	Values found by proposed method[a] (μg g^{-1})	Value of *t*-test[b]
SRM 1641d	1.56 ± 0.02	1.45 ± 0.15	1.35

[a] Mean value ± standard deviation, $N = 3$. [b] At 95% confidence level.

Table 3 Determination of Hg(II) ions in real samples using polymeric CN packed column. (Column parameters: pH 6.0, sample flow rate 8 mL min^{-1}, sample volume 1 L; eluent volume 5 mL (0.5 M HCl) and eluent flow rate 1 mL min^{-1})

Samples	Amount added (μg)	Amount found (μg L^{-1}) ± standard deviation[a]	Recovery percent of spiked amount[c] (RSD)	Value of *t*-test[d]
Tap water	0	ND[b]	—	—
	3	2.99 ± 0.06	99.3 (0.65)	0.26
	5	5.04 ± 0.16	100.8 (1.34)	1.43
Sea water	0	2.3 ± 0.46	—	1.12
	3	5.4 ± 0.59	100.2 (2.07)	1.55
	5	7.3 ± 0.52	100 (2.23)	2.68
Ground water	0	ND[b]	—	—
	3	2.88 ± 0.30	98.3 (0.45)	1.88
	5	5.01 ± 0.56	100.4 (1.26)	2.08

[a] $N = 3$. [b] Not detected. [c] Relative standard deviation. [d] At 95% confidence level, $t_{critical} = 4.303$.

Table 4 Analytical figures of merits of prepared sorbent and other reported sorbents[a]

Sorbent	Adsorption Capacity (mg g^{-1})	PF	DL (μg L^{-1})	Technique	Ref.
g-C_3N_4	180	200	0.6	ICP-OES	This work
PAN-C_3N_4 @COFs	25.48	—	1.76	—	34
Polypyrole@g-C_3N_4	197	—	—	ICP-OES	35
ZnSe/g-C_3N_4	16.59	—	—	ICP-AES	36
CN@ZrO_2	180	640	0.05	ICP-OES	37
AAO-PAP	360	933	0.02	ICP-OES	38

[a] PF – preconcentration factor; DL – detection limit.

summary, the validation results indicate that the proposed preconcentration and analytical technique using the CN-packed column is accurate, sensitive, and precise for the determination of Hg(II) in real environmental samples. Further, a comparative data of analytical characteristics of the prepared sorbent with other reported sorbents has been given in Table 4. It was observed that the prepared sorbent shows comparable statistics and can be utilized in the preconcentration and determination of trace Hg(II) ions.

3.7. Selectivity studies

The hinderance by other heavy metal ions, such as Co(II), Zn(II), Pb(II), Cd(II), Cu(II), and Ni(II), on the adsorption of Hg(II) were studied. To do this a sample solution contain Hg(II) ions and other heavy metals were pass through the adsorbent packed column. The sample volume was 50 mL, with Hg(II) concentration set at 10 μg L^{-1}, and the concentrations of other metal ions were varied between 50 μg L^{-1} and 100 μg L^{-1}. The concentration of Hg(II) was assessed using ICP-OES after elution of the sorbed Hg(II). Fig. 8 presents the findings, and it was observed that the CN sorbent exhibits low sorption for other competing divalent metal ions, except for Cu(II). The tolerance limit was established as the highest concentration of co-ions that caused a variation of less than 5% in the recovery of Hg(II). For all the added ions, the analyte recovery of Hg(II) ranged from 96% to 99%, indicating no appreciable

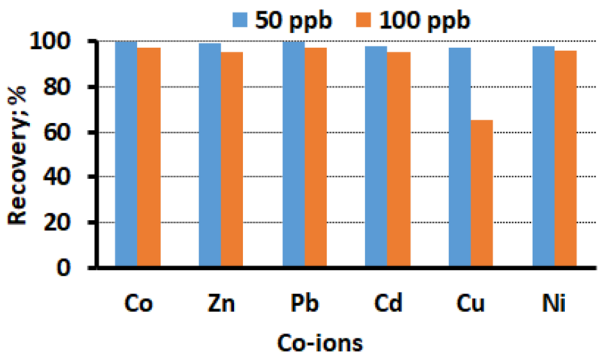

Fig. 8 Effect of divalent co-ions on the adsorption and recovery of Hg(II) (sample volume 50 mL, Hg(II) concentration 10 μg L^{-1}, pH 6.0, flow rate 8 mL min^{-1}).

interferences in the sorption and measurement of Hg(II). The results suggest that the CN sorbent has a preference for the selective sorption of Hg(II) over other divalent metal ions. The selective adsorption of Hg(II) is might be due the strong chelate forming capability of –N atom of CN with the Hg(II). Since both are classified as soft acid and soft base, in the classical parsons HSAB theory. In conclusion, under optimized experimental conditions, effective recovery of Hg(II) in the presence of other heavy metal ions in the concentration range of up to 100 $\mu g\ L^{-1}$, except for Cu(II), is possible, allowing for quantitative measurement. Cu(II) concentrations above 50 $\mu g\ L^{-1}$ was found to interfere in the adsorption of Hg(II) under competitive conditions (Fig. 8). Overall, the study demonstrates the selectivity of the CN sorbent for the sorption of Hg(II) over other divalent metal ions, making it a promising approach for the preconcentration and determination of Hg(II) in the presence of common heavy metal co-ions in environmental samples.

4. Conclusion

The study focused on optimizing the use of polymeric carbon nitride sheets in the column technique for the preconcentration and detection of trace Hg(II) in actual samples. The approach aimed to selectively extract Hg(II) in the presence of other co-existing ions commonly found in environmental samples. The high selectivity and excellent affinity of the polymeric carbon nitride sheets for Hg(II) were attributed to the soft–soft interaction between the N atom and Hg(II). The suggested solid-phase extraction (SPE) approach proved to be effective enough for quantitatively assessing trace levels of Hg(II) in real water samples at ppb ($\mu g\ L^{-1}$) scale, even in the presence of other common co-existing ions. The soft–soft interaction with Hg(II) ensured that the polymeric carbon nitride selectively adsorbed Hg(II) without interference from other ions, enabling accurate and reliable measurements. The application of the optimized SPE technique was further validated by examining Standard Reference Material and using the standard addition procedure. This verification process confirmed the accuracy and reliability of the proposed approach for the determination of trace Hg(II) in environmental samples. The study's findings demonstrate the potential of using polymeric carbon nitride sheets in SPE as a promising sorbent for monitoring and evaluating environmental samples. This approach opens up possibilities for the adoption of additional nanomaterials as potential sorbents in environmental monitoring and analysis. In conclusion, the optimized column technique using polymeric carbon nitride sheets showed high selectivity and efficiency for extracting trace Hg(II) from real water samples. The method's accuracy and reliability were confirmed through validation with Standard Reference Material and standard addition procedures. The application of CN in SPE could pave the way for exploring other nanomaterials as potential sorbents in environmental monitoring and analysis.

Conflicts of interest

There is no conflict of interest.

Acknowledgements

This project was supported by Researchers Supporting Project number (RSP2023R400), King Saud University (Riyadh, Saudi Arabia).

References

1 P. A. Rodrigues, *et al.*, Mercury contamination in seafood from an aquatic environment impacted by anthropic activity: seasonality and human health risk, *Environ. Sci. Pollut. Res. Int.*, 2023, **30**, 85390–85404.
2 K. Zhang, *et al.*, Mercury reduction by black carbon under dark conditions, *Water Res.*, 2023, **242**, 120241.
3 Z. Tang, *et al.*, Ecological risk assessment of aquatic organisms induced by heavy metals in the estuarine waters of the Pearl River, *Sci. Rep.*, 2023, **13**(1), 9145.
4 Z. Y. Yan, *et al.*, [Safety evaluation of Tibetan medicine Qishiwei Zhenzhu Pills based on serum pharmacochemistry and network pharmacology], *Zhongguo Zhong Yao Za Zhi*, 2023, **48**(9), 2538–2551.
5 U. Lopez-Gonzalez, *et al.*, Exposure to mercury among Spanish adolescents: Eleven years of follow-up, *Environ. Res.*, 2023, **231**(Pt 2), 116204.
6 J. A. Camacho, *et al.*, Reproductive-Toxicity-Related Endpoints in C. elegans Are Consistent with Reduced Concern for Dimethylarsinic Acid Exposure Relative to Inorganic Arsenic, *J. Dev. Biol.*, 2023, **11**(2), 1–8.
7 M. Silva-Gigante, *et al.*, Heavy metals and metalloids accumulation in common beans (Phaseolus vulgaris L.): a review, *Chemosphere*, 2023, **335**, 139010.
8 Y. Takanezawa, *et al.*, Proteasome and p62/SQSTM1 are involved in methylmercury toxicity mitigation in mouse embryonic fibroblast cells, *J. Toxicol. Sci.*, 2023, **48**(6), 355–361.
9 F. Hanis, *et al.*, Analysis and Risk Assessment of Essential and Toxic Elements in Algerian Canned Tuna Fish, *Biol. Trace Elem. Res.*, 2023, DOI: **10.1007/s12011-023-03735-8**.
10 L. Li, *et al.*, A triphenylamine-based fluorescent probe with phenylboronic acid for highly selective detection of Hg(2+) and CH(3)Hg(+) in groundwater, *Org. Biomol. Chem.*, 2023, **21**, 5560–5566.
11 A. H. Al-Bagawi, *et al.*, A simple and low cost dual-wavelength beta-correction spectrophotometric determination and speciation of mercury(II) in water using chromogenic reagent 4-(2-thiazolylazo) resorcinol, *Spectrochim. Acta, Part A*, 2017, **187**, 174–180.
12 L. Cheng, *et al.*, Highly efficient electrochemical gas reduction on a three-dimensional foam electrode: mechanism and application for the determination of hazardous mercury in complex matrix, *Mikrochim. Acta*, 2020, **187**(9), 517.
13 M. W. Tehrani, K. X. Yang and P. J. Parsons, Development and characterization of reference materials for trace element analysis of keratinized matrices, *Anal. Bioanal. Chem.*, 2020, **412**(8), 1847–1861.

14 A. Atasoy Aydin, *et al.*, Method development, validation, and application for simultaneous determination of 56 new psychoactive substances in surface water by LC-MS/MS, *Environ. Sci. Pollut. Res. Int.*, 2023, **30**, 85920–85929.
15 A. A. Fathi, *et al.*, Selective extraction of apixaban from plasma by dispersive solid-phase microextraction using magnetic metal organic framework combined with molecularly imprinted polymer nanocomposite, *J. Sep. Sci.*, 2023, e2201055.
16 Y. Y. Gao, *et al.*, [Recent application advances of covalent organic frameworks for solid-phase extraction], *Se Pu*, 2023, **41**(7), 545–553.
17 J. Liu, *et al.*, Extraction methods and compositions of polyphenols in Shanxi aged vinegar, *J. Chromatogr. A*, 2023, **1705**, 464169.
18 G. A. Toader, F. R. Nitu and M. Ionita, Graphene Oxide/Nitrocellulose Non-Covalent Hybrid as Solid Phase for Oligo-DNA Extraction from Complex Medium, *Molecules*, 2023, **28**(12), 1–10.
19 Y. Zhang, Y. Huang and X. Huang, One-pot fabrication of magnetic adsorbent based on polymeric ionic liquid/aminated carbon nanotubes composite for efficient capture of synthetic auxins in complex samples prior to chromatographic analysis, *J. Sep. Sci.*, 2023, e2300250.
20 Y. Zhong, *et al.*, Application of wastewater-based epidemiology to estimate the usage of betaagonists in 31 cities in China, *Sci. Total Environ.*, 2023, **894**, 164956.
21 B. Mishra, N. Arya and S. Tiwari, Investigation of formulation variables affecting the properties of lamotrigine nanosuspension using fractional factorial design, *Daru*, 2010, **18**(1), 1–8.
22 A. J. J, *et al.*, Biomimetic strategies to design metallic proteins for detoxification of hazardous heavy metal, *J. Hazard. Mater.*, 2018, **358**, 92–100.
23 E. G. K, *et al.*, Estimating the Absorbed Dose of Organs in Pediatric Imaging of (99m)Tc-DTPATc-DTPA Radiopharmaceutical using MIRDOSE Software, *J. Biomed. Phys. Eng.*, 2019, **9**(3), 285–294.
24 J. Lukose, *et al.*, Laser Raman tweezer spectroscopy to explore the bisphenol A-induced changes in human erythrocytes, *RSC Adv.*, 2019, **9**(28), 15933–15940.
25 M. N, *et al.*, Adsorption of ciprofloxacin from aqueous solution using surface improved tamarind shell as an economical and effective adsorbent, *Int. J. Phytoremediation*, 2022, **24**(3), 224–234.
26 S. Singh, *et al.*, Removal of Pb ions using green Co(3)O(4) nanoparticles: Simulation, modeling, adsorption, and biological studies, *Environ. Res.*, 2023, **222**, 115335.
27 S. Singh, *et al.*, Applicability of new sustainable and efficient green metal-based nanoparticles for removal of Cr(VI): Adsorption anti-microbial, and DFT studies, *Environ. Pollut.*, 2023, **320**, 121105.
28 J. Yang, *et al.*, Defective polymeric carbon nitride: Fabrications, photocatalytic applications and perspectives, *Chem. Eng. J.*, 2022, **427**, 130991.
29 F. K. Kessler, *et al.*, Functional carbon nitride materials — design strategies for electrochemical devices, *Nat. Rev. Mater.*, 2017, **2**(6), 17030.
30 I. F. Teixeira, *et al.*, Carbon nitrides and metal nanoparticles: from controlled synthesis to design principles for improved photocatalysis, *Chem. Soc. Rev.*, 2018, **47**(20), 7783–7817.
31 D. M. Haiber, *et al.*, In-Plane Structural Fluctuations in Differently Condensed Graphitic Carbon Nitrides, *Chem. Mater.*, 2021, **33**(1), 195–204.
32 R. Mohini and N. Lakshminarasimhan, Coupled semiconductor nanocomposite g-C3N4/TiO2 with enhanced visible light photocatalytic activity, *Mater. Res. Bull.*, 2016, **76**, 370–375.
33 F. Chang, *et al.*, Fabrication, characterization, and photocatalytic performance of exfoliated g-C3N4–TiO2 hybrids, *Appl. Surf. Sci.*, 2014, **311**, 574–581.
34 C. Yang, *et al.*, Multifunctional 3D PAN-C3N4@COFs for efficiently dynamic and static adsorption of mercury and its chemometric detection, *Process Saf. Environ. Prot.*, 2023, **177**, 496–506.
35 M. A. Diab, *et al.*, Design of multifunctional 1D/2D polypyrrole nanotubes@pg-C3N4 binary nanocomposite for removal of mercury (Hg2+) from wastewater and supercapacitor applications, *J. Ind. Eng. Chem.*, 2023, **130**, 494–509.
36 H. Liu, *et al.*, Rational design via surface engineering on dual 2-dimensional ZnSe/g-C3N4 heterojunction for efficient sequestration of elemental mercury, *Chem. Eng. J.*, 2022, **448**, 137606.
37 H. Ahmad, *et al.*, Cellulose Nanofibers@ZrO2 membrane for the separation of Hg(II) from aqueous media, *J. Phys. Chem. Solids*, 2022, **168**, 110812.
38 H. Ahmad, B. H. Koo and R. A. Khan, Enrichment of trace Hg(II) ions from food and water samples after solid phase extraction combined with ICP-OES determination, *Microchem. J.*, 2022, **175**, 107179.